Journal of Science: Advanced Materials and Devices 9 (2024) 100801

Contents lists available at ScienceDirect

Journal of Science: Advanced Materials and Devices

journal homepage: www.elsevier.com/locate/jsamd

Research Article

Effect of Triton X-100 surfactant concentration on the wettability of polyethylene-based separators used in supercapacitors

S.M.B. Dissanayake [a,b], I.G.K.J. Wimalasena [a,b], N.M. Keppetipola [c], B.C. Karunarathne [a,b], A.D.T. Medagedara [a,b], Ludmila Cojocaru [c], Satoshi Uchida [d], R.M.G. Rajapakse [e], Kirthi Tennakone [a], Masamichi Yoshimura [f], G.R.A. Kumara [a,*]

[a] National Institute of Fundamental Studies, Hantana Road, Kandy, Sri Lanka
[b] Postgraduate Institute of Science, University of Peradeniya, Sri Lanka
[c] Université de Bordeaux, Institut des Sciences Moléculaires, UMR 5255 CNRS, 351 Cours de la Libération, F-33405, Talence Cedex, France
[d] The University of Tokyo, Research Center for Advanced Science and Technology (RCAST), 4-6-1, Komaba, Meguro, Tokyo, 153-8904, Japan
[e] Department of Chemistry, Faculty of Science, University of Peradeniya Sri Lanka, Sri Lanka
[f] Graduate School of Engineering, Toyota Technological Institute, 2-12-1 Hisakata, Tempaku, Nagoya, 468-8511, Japan

ARTICLE INFO

Keywords:
Supercapacitor
Polyethylene separator
Aqueous electrolyte
Triton X-100

ABSTRACT

Polyethylene-based separators are generally unsuitable for aqueous supercapacitors due to their poor wettability with the electrolyte, which impedes ion transport. However, incorporating Triton X-100 (2-[4-(2,4,4-trimethylpentan-2-yl)phenoxy]ethanol) into the aqueous sulfuric acid (H_2SO_4) electrolyte improves the wettability of polyethylene and facilitates ionic movement through its pores. In this study, Triton X-100 was added to 1.0 M H_2SO_4 at various concentrations (0.122%–1.210% V/V) to evaluate its impact on supercapacitor performance. Supercapacitors were assembled using activated carbon-filled carbon cloth electrodes, each of the above electrolytes and polyethylene sheet separators. Scanning electron microscopy revealed that the carbon cloth exhibited a uniform fiber distribution and high surface area for activated carbon integration. The polyethylene separator displayed a porous structure with an average pore size of 165 ± 35 nm. Triton X-100 significantly reduced the water contact angle from 101.5° (without surfactant) to 30.2° (with 1.21% V/V Triton X-100), enhancing polyethylene's wettability. This change from hydrophobic to hydrophilic characteristics enabled the formation of an electrical double layer at the separator/electrolyte interface, improving ionic transport. However, higher Triton X-100 concentrations increased the electrolyte's viscosity, which impeded ion movement. The highest specific capacitance of 55.3 F/g (at a scan rate of 0.005 V s^{-1}) was achieved with 0.488% V/V Triton X-100. The specific capacitance varied with surfactant concentration in a complex manner, influenced by micelle formation and precipitation. These findings were corroborated by cyclic voltammetry and AC impedance spectroscopy.

1. Introduction

Supercapacitors are constituted of two porous carbon electrodes impregnated with an electrolyte, sandwiching a separator [1]. The separator is essential to the device's operation as it insulates the two electrodes while allowing the electrolyte to penetrate. Its primary function is to prevent short-circuiting between the electrodes while permitting ionic transport [2–4]. Consequently, the separator material needs to be an electronic insulator that is permeable to ions. Most separators are made from polymeric materials such as polyethylene (PE), polypropylene, poly(vinylidene fluoride) (PVDF), and polytetrafluoroethylene (PTFE) [5–8]. These polymer separators are valued for their chemical stability, low interfacial resistance, thermal stability, and good mechanical strength [9].

For effective ion transport, the separator material must exhibit good wettability with water. The wettability of a separator mesh is influenced by the material's nature, pore size and shape, and the liquid's surface tension [10–12]. However, many commercial polymer separators suffer

Peer review under responsibility of Vietnam National University, Hanoi.
* Corresponding author.
E-mail address: kumara.as@nifs.ac.lk (G.R.A. Kumara).

https://doi.org/10.1016/j.jsamd.2024.100801
Received 18 July 2024; Received in revised form 1 October 2024; Accepted 7 October 2024
Available online 9 October 2024

from low hydrophilicity on their surfaces in contact with aqueous electrolytes, resulting in poor liquid retention and electrolyte absorption [13]. This limitation hinders ionic transport and adversely affects specific capacitance and charge-discharge characteristics. To enhance wettability, the surface energy of the polymer in contact with the electrolyte should be reduced. This can be achieved through the use of surface-active materials or surfactants. The high surface tension of water is due to the strong cohesive forces between its molecules [14]. Surfactants lower the surface tension, thereby improving the compatibility between hydrophilic aqueous electrolyte components and hydrophobic polymers. Surfactants feature polar head groups that interact with the polar substances in the electrolyte and non-polar hydrocarbon or fluorocarbon chains that interact with the hydrophobic polymer parts. This interaction facilitates the compatibility of the two materials, allowing ions to pass more easily through the polymer sheet. Consequently, this reduces the internal resistance of the separator membrane, thereby enhancing the capacitance, energy density, and power density of the supercapacitor [15].

Various methods have been employed to enhance the wettability of separators, thereby increasing ion permeation. For instance, Szubzda et al. improved the wettability and reduced the internal resistance of polyamide and polyethylene (PE) polymer separators by using low-energy plasma irradiation [11]. Similarly, Keppetipola et al. applied ozone (O_3) treatment to PE separators to enhance wettability and improve the storage properties of supercapacitors [10]. These treatments introduce surface-active sites by breaking chemical bonds, which generates free radicals or ions. Once exposed to water, these species react to form hydroxyl (OH) and hydrogen (H) groups [16,17]. Adequate introduction of –OH groups can significantly improve the surface hydrophilicity. However, these treatment methods can be costly and may require frequent application.

Therefore, exploring cost-effective surface treatment technologies for polymer separators is crucial to enhance wettability and reduce resistance, ultimately improving device performance. In this study, we demonstrate that hydrophobic PE separators can be rendered wettable and ion-permeable through the incorporation of the surfactant Triton X-100 (2-[4-(2,4,4-trimethylpentan-2-yl)phenoxy]ethanol). Triton X-100 is a non-ionic surfactant featuring a polar group with neutral ether and hydroxyl functionalities, and a non-polar chain composed of a 2-[4-(2,4,4-trimethylpentan-2-yl)phenyl group. The large non-polar group of Triton X-100 enhances hydrophobic interactions with the non-polar PE polymer, facilitating its attachment to the polymer surface, while the polar –O and -OH functionalities support cation hopping [18].

Unlike cationic surfactants, which could bind sulfate ions present in the electrolyte, Triton X-100 does not interfere with these ions due to its non-ionic nature. Anionic surfactants are also unsuitable as they may form strongly bound $–SO_3H$ or –COOH groups. Hence, Triton X-100, a widely used and readily available non-ionic surfactant, is chosen for this research. This paper details the significant performance improvements in supercapacitors comprising porous conducting carbon cloth pressed onto titanium plate electrodes, an aqueous H_2SO_4 electrolyte with Triton X-100, and a PE separator.

Therefore, the best choice is the use of a non-ionic surfactant, and Triton X-100 is a widely used and readily available non-ionic surfactant. It has been chosen as the most appropriate surfactant for this research due to its well-documented effectiveness in various applications. Triton X-100 has been extensively studied for its role in enhancing wettability and performance across different domains. For instance, in the field of colloid and polymer science, its application has been explored for improving dispersion stability and polymerization processes [19]. In biological macromolecules, Triton X-100 is utilized for its ability to solubilize proteins and other macromolecules [20]. Its utility extends to chemical applications where it aids in modifying surface properties and enhancing reaction efficiencies [21]. Additionally, in molecular physics, Triton X-100 has been examined for its effects on molecular interactions and material properties [22]. Recent studies in colloids and surfaces highlight its role in optimizing surfactant formulations for various industrial processes [23,24], while research in molecular liquids demonstrates its influence on liquid structure and behavior [25]. These applications underline the versatility and effectiveness of Triton X-100 in various arenas, making it an ideal choice for our research on supercapacitors.

Recent advancements in supercapacitor separators have explored various materials beyond traditional polymers, including graphene-based and ceramic separators, which offer improved ionic conductivity and mechanical strength [23–25]. For instance, flexible and high-performance supercapacitors with nanostructured separator materials have shown notable improvements [26–28]. Additionally, surface modification techniques such as chemical etching, plasma treatments, and grafting have been employed to enhance wettability, with significant performance improvements reported [28–31].

The role of surfactants in energy storage devices has also been investigated extensively. Surfactants like Triton X-100 have demonstrated promise in enhancing the wettability and ionic conductivity of separators, with broader studies examining their impact on batteries and fuel cells [32–34]. Comparative studies underscore the effectiveness of non-ionic surfactants in maintaining compatibility with aqueous electrolytes while avoiding interference with ion transport [28–30].

Economic and practical considerations are crucial in developing of cost-effective and sustainable technologies. Research has focused on scalable and environmentally friendly practices for material selection and surface treatments [34–36]. Furthermore, performance metrics such as capacitance, energy density, and cycle life have been extensively evaluated, showcasing the benefits of improved separator materials across various applications [36,37]. Real-world applications of these technologies continue to expand, highlighting their relevance in modern energy storage systems [37,38].

2. Experimental

2.1. Preparation of the electrodes and the fabrication of the supercapacitor

Supercapacitor electrodes were made by porous conducting carbon cloth (3 mm thick) pressed onto titanium plates (2 cm × 4 cm). The pore structure of the carbon cloth is compacted with powdered activated coconut charcoal via the following procedure: charcoal powder (grain size 2–3 μm, FE-SEM JSM6700F, Jeol 6700F) dispersed in isopropanol was introduced dropwise into the carbon cloth (Ningbo Vet Energy Technology Co., Ltd.) electrodes placed on a hot plate (70 °C) for 10 min until the surface is leveled after intermittent pressing. A PE separator (SETELA, Toray Industries Inc, thickness of 7 μm) was sandwiched between the electrodes impregnated with 1 M H_2SO_4 (Sigma Aldrich, USA, Assay 98.0%) containing various amounts of non-ionic surfactant Triton X-100 (Sigma Aldrich, USA, Assay 97.7%). The concentrations of Triton-X-100 used are in terms of V/V% 0.122, 0.244, 0.366, 0.488, 0.609, 0.730, 0.970 and 1.210, respectively.

2.2. Electrochemical analyzing

The values of the capacitance of the supercapacitors at different scanning rates were determined by cyclic voltammetry (Metrohm Autolab PGSTAT 128 N) in a two-electrode configuration. The specific capacitance values in Farads per gram (F g^{-1}) of the fabricated supercapacitors were determined from the CV by integrating the charging-discharging curves in the potential range 0–1 V. The electrochemical impedance studies were performed with the same system but using the FRA software. The Nyquist plots obtained were fitted to the equivalent circuit using the built-in NOVA software.

2.3. Viscosity and contact angle measurements

The viscosity of the electrolyte at corresponding concentrations of the surfactant of the same molarity of H_2SO_4 was measured using an Ubbelohde (ASTM) viscometer at 29 °C. Porosity was calculated from apparent and true density values. The true density was obtained by helium pycnometer using an AccuPyc 1340 pycnometer (Micromeritics). Apparent density was calculated from the weight and volume measurements of the sample. Contact angle measurements were conducted using the Kruss DSA100 goniometer with 3 μL droplets. Each contact angle represents an average of 5 samples. Calibration ensured precise planar alignment before each session. The Young-Laplace model was applied for analysis, with repeated measurements confirming consistency. Multiple locations were assessed to ensure uniform surface flatness, ensuring measurement reliability and accuracy.

2.4. Morphological study

The scanning electron microscopic (SEM) images of the carbon cloth, electrodes, and separator were analyzed using a field emission scanning microscope (FE-SEM JSM6700F, Jeol 6700F).

3. Results and discussion

The SEM images of the electrodes, including carbon fibers, carbon fibers filled with activated carbon, and the surface of the PE separator used in this work, are shown in Fig. 1. Fig. 1(a) depicts the carbon cloth, which consists of uniform carbon microfibers. This morphology provides a high surface area for use as current collectors in supercapacitor electrodes, offering advantages over traditional flat metal current collectors. The porous structure of the carbon cloth facilitates the incorporation of activated charcoal grains into its pores, as illustrated in Fig. 1(b). Additionally, the PE separator, shown in Fig. 1(c), exhibits a porous structure with an estimated pore size of 165 ± 35 nm, indicating a relatively uniform pore size distribution. This porosity is beneficial as it allows stable ionic transport between electrodes, contributing to higher efficiency and improved cycling lifetime of the supercapacitor.

The electrochemical characterization of the supercapacitors was conducted using a two-electrode configuration as detailed in the experimental section. The specific capacitance of the system was calculated using Equation (1) [39].

$$C = \frac{1 \int IdV}{2m\Delta V \frac{dV}{dt}} \quad (1)$$

where m is the mass of the activated carbon layer on the electrode surface, I is current, ΔV is the potential range used and dV/dt is the potential scan rate used for the CV experiment.

The supercapacitor's storage capability was evaluated using a device configured with two carbon electrodes separated by a PE separator and filled with an H_2SO_4 electrolyte. To investigate the effect of surfactant addition, varying amounts of Triton X-100 were mixed into the electrolyte. Initially, with a PE separator and aqueous 1 M H_2SO_4 electrolyte without Triton X-100, the supercapacitor exhibited no measurable capacitance. This lack of capacitance is attributed to the PE separator not being wetted by the electrolyte, which inhibits the formation of the electrical double layer at the separator/electrolyte interface. Without the electrical double layer, ionic communication across the separator is impeded, negatively affecting supercapacitor performance.

To address this issue, Triton X-100 was introduced as a surfactant to enhance the formation of the electrical double layer at the electrode/electrolyte interface. The effect of Triton X-100 was studied by evaluating the specific capacitance of the supercapacitor with various concentrations of the surfactant at scan rates of 0.005, 0.010, and 0.020 V s^{-1}. The results, presented in Fig. 2, cover an intermediate range of scan rates that provide a balanced view of the electrochemical behavior, avoiding the extremes of very slow or very fast rates that could either obscure kinetic processes or introduce significant capacitive currents.

As the surfactant concentration increases, the capacitance of the supercapacitor initially rises, reaching a peak value of 55.3 F/g at a Triton X-100 concentration of 0.488% (V/V) in the electrolyte. Beyond this optimal concentration, however, the capacitance begins to decrease as the surfactant concentration continues to rise, reaching up to 70% (V/V) at each scan rate. Notably, the capacitance exhibits a more complex variation pattern at higher concentrations, showing another maximum at 0.970% (V/V).

The initial increase in specific capacitance with increasing Triton X-

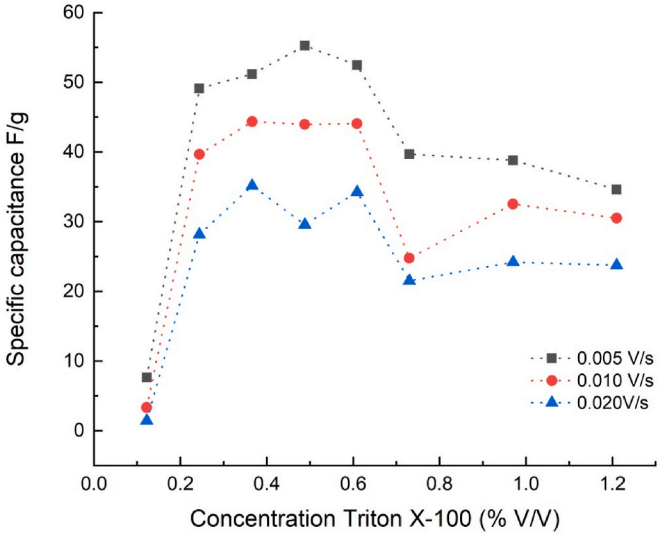

Fig. 2. The specific capacitance values of the Ti/C/H_2SO_4(aq, 1 M)/polyethylene separator/H_2SO_4(aq)/C/Ti supercapacitor with different amounts of Triton X-100 in the electrolyte.

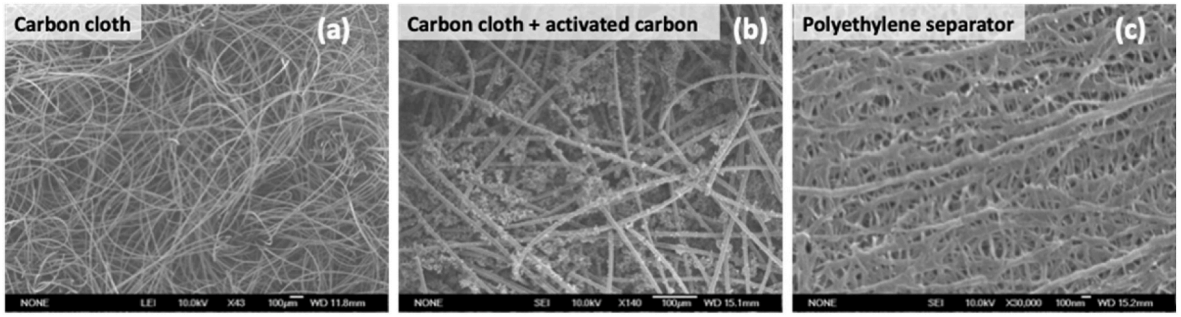

Fig. 1. The SEM images of the components of the supercapacitor; (a) porous carbon cloth, (b) activated carbon powder on the porous carbon cloth, and (c) PE separator.

100 concentration is attributed to the enhanced formation of the electrical double layer at the separator/electrolyte interface, which facilitates ionic migration across the membrane. However, as the concentration of Triton X-100 increases, the PE surface becomes saturated with surfactant molecules. When the concentration surpasses the critical micelle concentration, surfactant molecules aggregate into micelles, as shown in Fig. 3. These micelles significantly increase the viscosity of the electrolyte, which in turn reduces ion mobility. Since ion mobility is directly related to ionic conductivity, the decreased ionic conductivity results in a reduced specific capacitance.

Additionally, for non-ionic surfactants like Triton X-100, the cloud point indicates the formation of cloudiness in the electrolyte due to micelle aggregation. As the surfactant concentration rises further, these cloudy micelles can aggregate and form precipitates. The variation in contact angle with increasing surfactant concentration can be explained by the surfactant's role in reducing surface tension. Triton X-100 decreases the surface tension of water, enhancing the compatibility between the hydrophilic aqueous electrolyte and the hydrophobic polymer surfaces. As the surfactant concentration increases, surface tension decreases, leading to a lower contact angle and indicating improved wettability.

As the surfactant concentration increases, the formation of micelles initially leads to a decrease in electrolyte viscosity, which in turn enhances ionic transport. This effect contributes to the observed second increase in capacitance after reaching 0.733% (V/V) Triton X-100. However, as the surfactant concentration continues to rise, micellization resumes, leading to higher viscosity and reduced ionic transport, as evidenced by the decrease in specific capacitance at each scan rate.

The points of micellization and precipitation are directly related to the surfactant concentration and are consistent across all scan rates, as supported by the trend shown in Fig. 4(a), which depicts the variation in relative viscosity with Triton X-100 concentration. Initially, from 0 to 0.488% (V/V), the increase in relative viscosity due to surfactant addition could impede ion transport. Nonetheless, the enhanced hydrophilicity of the PE separator facilitates ion transport across the membrane, improving overall device performance and increasing specific capacitance up to this concentration.

Beyond 0.488% (V/V), the rapid increase in viscosity up to 0.733% (V/V) due to the formation of stable micelles outweighs the benefits of improved hydrophilicity, resulting in decreased specific capacitance. After this point, up to 0.970% (V/V), the increase in viscosity slows as micelles begin to precipitate gradually. This trend in viscosity closely aligns with the variation in specific capacitance observed in the device.

The direct evidence of the change in wettability of the PE surface due to Triton X-100 addition is illustrated in Fig. 4(b) and (c). These results confirm that the PE separator's surface transitions from hydrophobic to hydrophilic with the presence of Triton X-100. Specifically, the contact angle with water decreases from 101.5° to 30.2° when the electrolyte contains 1.21% (V/V) Triton X-100. Adding just 25 μL of Triton X-100 to the H_2SO_4 electrolyte reduces the contact angle from 99.1° to 37°, and further increases in Triton X-100 concentration result in only slight changes, stabilizing around 30°.

The minimal variation in the contact angle between 0.244% and 0.488% (V/V) Triton X-100 can be attributed to the behavior of surfactants at the liquid-air interface. Once a certain concentration threshold is reached, surfactant molecules saturate the surface, and additional increases in concentration have little effect on the contact angle, as the surface tension remains largely unchanged. Conversely, the specific capacitance exhibits significant fluctuations within this concentration range due to micelle formation.

Micelles initially form as surfactant concentration increases. In these aggregates, the hydrophilic heads of surfactant molecules face outward while the hydrophobic tails are shielded within the micelle core. Micelles, behaving somewhat like charged particles, can alter the electrical characteristics of the solution and initially enhance capacitance. However, at higher concentrations, the formation of larger micelles may not contribute positively to the system's total capacitance. These larger micelles can combine and aggregate, reducing overall capacitance, which contrasts with the expected improvements from smaller micelles. Additionally, changes in surfactant concentration can affect the solution's viscosity, indirectly impacting capacitance by altering the mobility and dispersion of charged species in the solution [40,41].

Based on these observations, an optimal Triton X-100 concentration of 0.488% (V/V) is recommended to achieve effective wettability of the PE separator with the electrolyte.

Fig. 5 shows the CV curves of the device with an optimum Triton X-100 concentration of 0.488 (% V/V) at three different scan rates (0.005 V s^{-1}, 0.010 V s^{-1}, and 0.020 V s^{-1}). The device demonstrates perfect capacitive behavior of constant current in a wide range of voltages when the scan rate is low (0.005 V s^{-1}). Although this trend of constant current regime gradually decreases when the scan rate is decreased, at least for the three scan rates used, there are not any redox peaks characteristic of Faradaic processes taking place at any electrode/electrolyte interface. Therefore, these currents can also be considered as capacitive currents. The reason for not having any redox peaks is that the carbon electrodes have very large overpotentials for both H^+ reduction and sulfate oxidation. The Triton X-100 used, and water molecules are also electroinactive within this potential range on the electrode surface. As such, any redox processes are happening in the device to decrease its performance with time. In other words, the constructed supercapacitor behaves as a pure capacitor in the voltage range investigated. This confirms that the device is only charging and discharging through the physical migration of ions and the incorporation of surfactant does not involve any side reactions or pseudocapacitive reactions.

The electrical behavior of the supercapacitor can be ascertained by AC impedance spectroscopy [42]. The Nyquist plot, the equivalent circuit that has the best fit to the Nyquist plot, and the Bode plots obtained for the supercapacitor with 0.488 (% V/V) and 0.366 (% V/V) Triton X-100 in 1 M H_2SO_4 electrolyte of the supercapacitor are shown in Fig. 6 (a and b), respectively. In each case, (i), (ii), (iii), and (iv) represent the

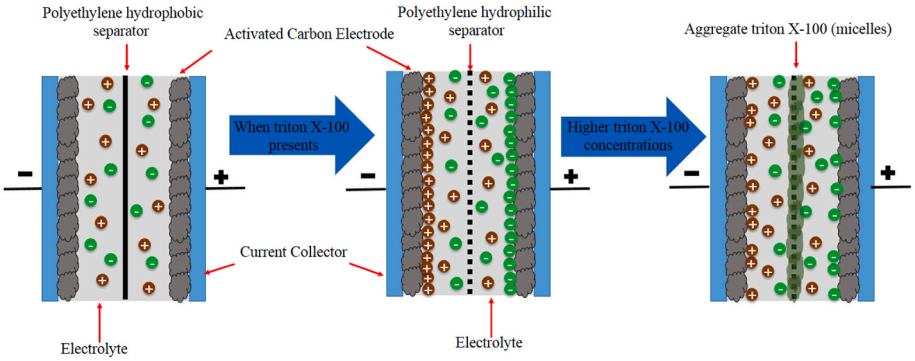

Fig. 3. Effect on the hydrophobic separator before and after the Triton X-100 treatment.

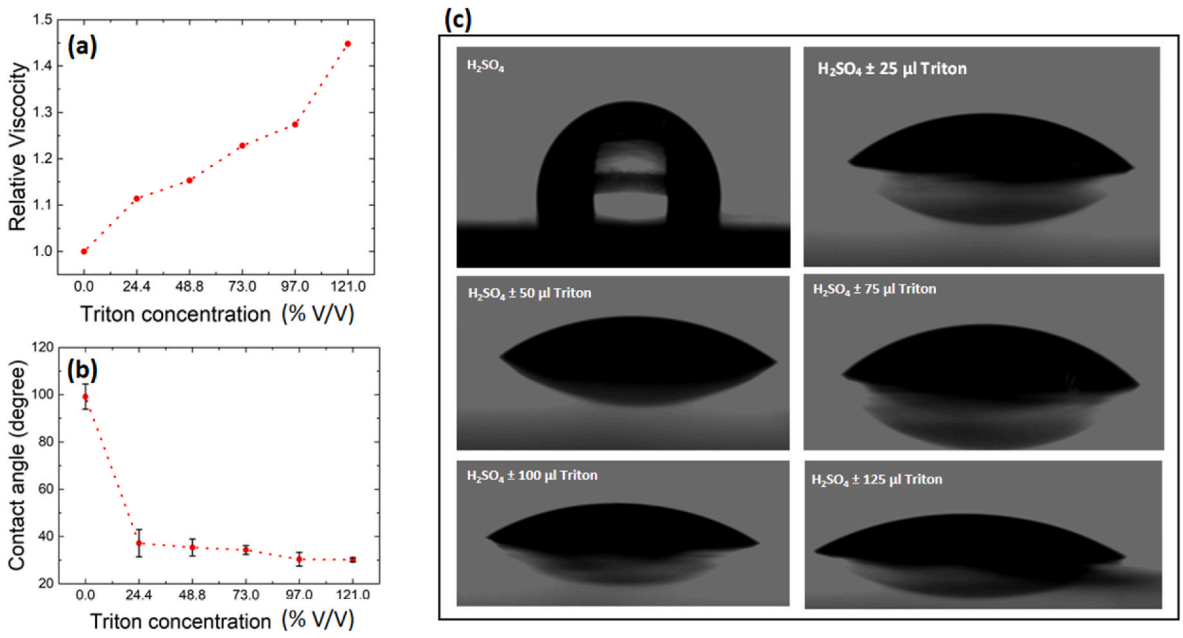

Fig. 4. The variation of the (a) relative viscosity, (b) contact angle of the electrolyte on the PE separator, and (c) images showing the wettability of the PE with H_2SO_4/Triton X-100 concentration.

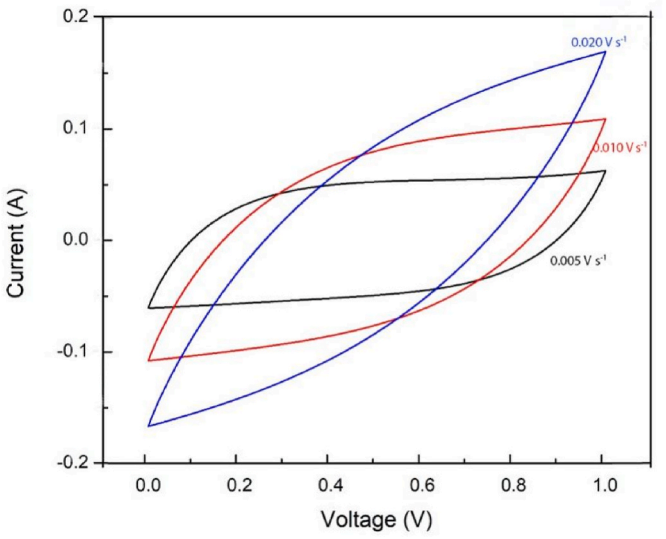

Fig. 5. Cyclic voltammograms at 0.005 V s^{-1}, 0.010 V s^{-1}, and 0.020 V s^{-1} scan rates corresponding to optimum surfactant concentration of 48.8 (% V/V).

Nyquist plot (real part of impedance, Z', versus the negative value of the imaginary part of the impedance, -Z''), equivalent circuit, the total impedance, Z, versus frequency, f, Bode plot and the phase versus frequency Bode plot, respectively. It consists of the highest frequency x-axis intercept representing the series resistance, R_s, of the device, a semicircle describing parallelly connected ion transport resistance in the electrical double layer formed at the electrode/electrolyte interface, R_{dl}. Double layer capacitance, C_{dl}, ~45° inclined straight line describing the Warburg impedance, W, corresponding to the electrolyte conductance, and a constant phase element, CPE, describing the ion conductance through the membrane and finally, an almost vertical line at the lowest frequency domain showing the overall capacitance, C, of the device. The Bode plots also show the presence of these circuit elements including constant phase elements in the device being studied. It is interesting to note that the optimum Triton X-100 concentration of 0.488 (% V/V) gave the highest specific capacitance in CV measurements and has the highest capacitance of 9.53 F. Since the mass of carbon material in each electrode is 0.162 g, the specific capacitance is 58.8 F/g, and is the same value as that obtained from CV measurements. The corresponding specific capacitance of the supercapacitor with its electrolyte containing 0.366 (% V/V) Triton X-100 is 35.7 F/g and is also close to that obtained in CV measurements. Interestingly, R_s at the optimum device is 340 mΩ but that in the other having a lower specific capacitance is 314 mΩ. This is possibly due to an increase in viscosity thus making the ion ingress and egress at the carbon/solution interface somewhat difficult when Triton X-100 concentration is increased though the change in magnitude is not very significant. That is reflected by the higher value of the ion transport resistance of the electrical double layer formed at the electrode/electrolyte interface, R_{dl}, where the corresponding values are 752 mΩ and 321 mΩ, respectively, for the optimum and the other device. The double layer capacitance, C_{dl}, also follows the same trend (For the supercapacitors having the optimum 0.488 (% V/V) Triton X-100, R_{dl} = 82.2 µF and that for the one with 0.366 (% V/V) Triton X-100 is 223 µF. However, the Warburg impedance due to ion transport in the optimized device is much higher but that of the other is not measurable. The ionic mobility across the membrane is determined by the constant phase element describing a conductance element. Its value for the optimized device is 1.31 mho (S) and that for the other device tested is 689 mmho (mS); a factor of 1.9 increase in the optimized device. This is clear evidence for the effect of Triton X-100 in inducing the hydrophilicity to the hydrophobic PE membrane enabling the ionic transport across the membrane. The device containing 0.488 (% V/V) Triton X-100 in the electrolyte has the highest specific capacitance and is due to its highest ionic conductance of the separator. Therefore, these results match well with those described by several other independent techniques described above. Overall, all these experimental results, points to conclusion that using a non-ionic surfactant such as Triton X-100 in the electrolyte, hydrophobic PE can be made hydrophilic to allow for ion transport through the pores of the membrane and therefore such a low-cost material could be used as a separators in supercapacitors. However, the effect of the concentration of the surfactant on the specific capacitance follows a complicated pattern that depends on many factors such as increased viscosity due to micelle formation at the critical micelle concentration, cloud point, and the precipitation of the micelles as

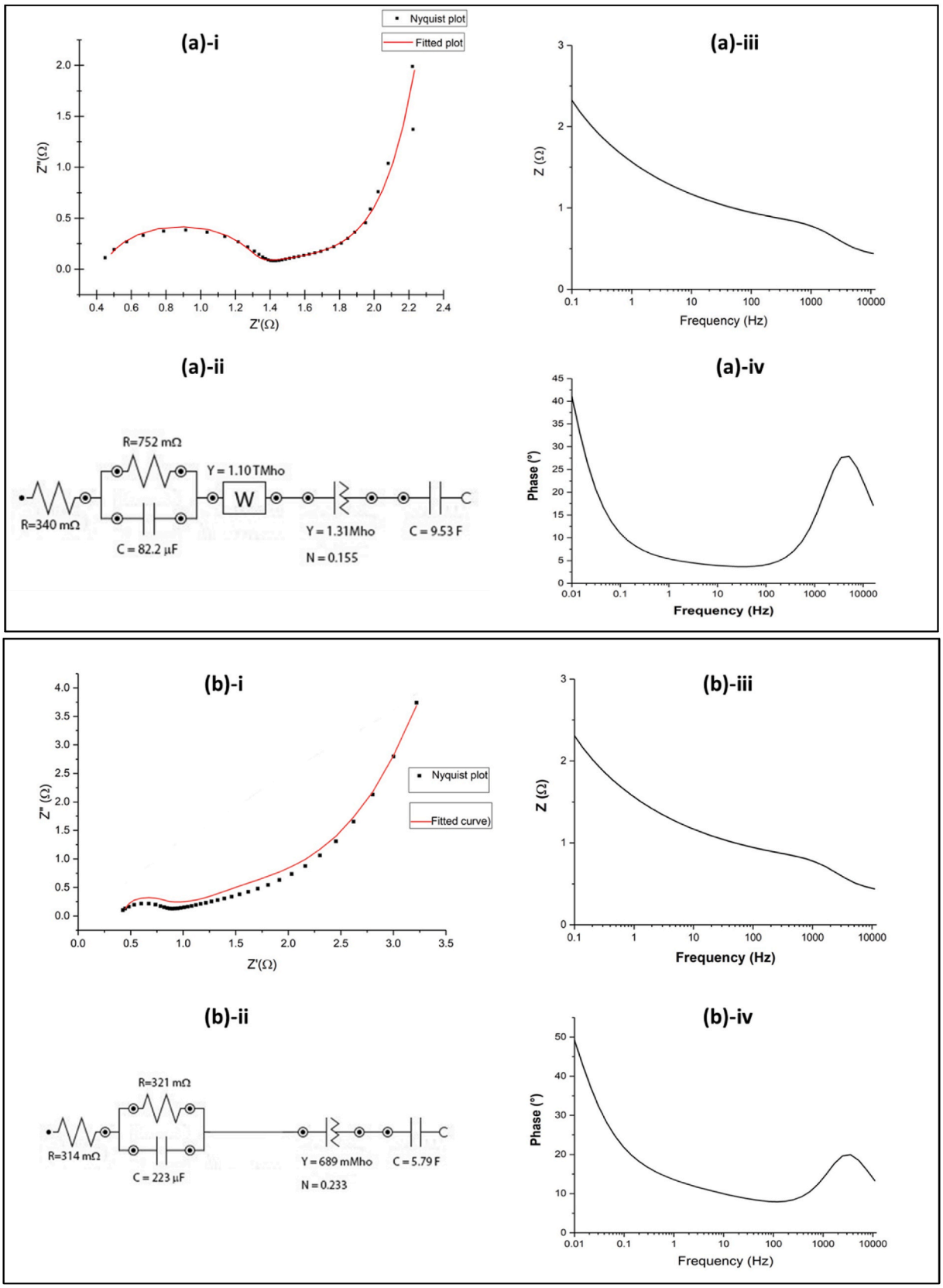

Fig. 6. (a) The (a–i) Nyquist plot (Real part of impedance, Z', versus the negative value of the imaginary part of the impedance, -Z''), (a-ii) equivalent circuit that has the best fit to the Nyquist plot, (a-iii) total impedance, Z, versus frequency, f, Bode plot (a-iv) the phase versus frequency Bode plot for the supercapacitor with an electrolyte containing 0.488 (% V/V) Triton X-100 non-ionic surfactant, (b) The (b–i) Nyquist plot (real part of impedance, Z', versus negative value of the imaginary part of the impedance, -Z''), (b-ii) equivalent circuit that has best fit to the Nyquist plot, (b-iii) total impedance, Z, versus frequency, f, Bode plot (b-iv) the phase versus frequency Bode plot for the supercapacitor with electrolyte containing 0.366 (% V/V) Triton X-100 non-ionic surfactant.

surfactant concentration is increased.

In our study, we observed a peak specific capacitance of 55.3 F g^{-1} at a Triton X-100 concentration of 0.488% (V/V), which is consistent with recent findings on surfactant-enhanced supercapacitors. Similar enhancements in performance with surfactant addition have been reported by Zhang et al. [35], who investigated the use of non-ionic surfactants to improve the wettability of electrode materials, resulting in increased capacitance and energy density. Our results also align with the observations of Liu et al. [28], who noted that the introduction of surfactants like Triton X-100 led to significant improvements in the ionic conductivity and overall performance of supercapacitors by facilitating the formation of an effective electrical double layer. Furthermore, the effect of surfactant concentration on viscosity and capacitance observed in our study parallels the findings of Huang et al. [7], who explored how micelle formation and precipitation at high surfactant concentrations can impede ion transport, thus decreasing capacitance. Our work extends these findings by providing a detailed examination of the interplay between surfactant concentration, viscosity, and capacitance across a range of concentrations. Additionally, our results contribute to the understanding of how a surfactant affects the wettability of polyethylene separators, a topic that has been less explored in the literature but is crucial for optimizing supercapacitor performance [21]. The observed fluctuations in specific capacitance with increasing surfactant concentration, including a secondary peak, offer new insights into the balance between enhanced wettability and increased viscosity, complementing and expanding upon existing studies in this area [22–25].

4. Conclusion

This work presents a significant advancement in utilizing electronically insulating and chemically resistant polyethylene separators in supercapacitors, which are typically non-wetted by aqueous electrolytes. By incorporating a non-ionic surfactant, Triton X-100, into the aqueous H_2SO_4 electrolyte, we have successfully improved the wettability and performance of the separators. Our findings indicate that an optimal surfactant concentration of 0.488% (V/V) Triton X-100 in the aqueous H_2SO_4 electrolyte yields the highest specific capacitance values across all scan rates tested, achieving a peak capacitance of 55.3 F g^{-1} at a scan rate of 0.005 V s^{-1}. Beyond this optimal concentration, increased surfactant levels result in higher electrolyte viscosity, which impedes ion transport and leads to decreased capacitance due to ion crossover and potential surfactant precipitation.

To further advance this research, exploring alternative non-ionic and ionic surfactants could provide additional improvements in wettability and performance. Additionally, a more detailed study on surfactant concentration over a broader range could offer a deeper understanding of the balance between enhanced wettability and increased viscosity. Long-term stability studies are also recommended to assess the durability and effectiveness of surfactant-treated separators under various operational conditions. Employing advanced characterization techniques, such as spectroscopy and microscopy, might provide further insights into the interactions between surfactants and separator materials at a molecular level.

From an industrial perspective, the findings suggest promising applications in developing high-performance supercapacitors with polyethylene separators, potentially benefiting energy storage devices in electronics, automotive, and renewable energy sectors. Furthermore, exploring cost-effective manufacturing processes for incorporating surfactant-treated separators into large-scale production could make these advanced supercapacitor technologies more accessible and economically viable. Overall, this research offers a foundation for enhancing polyethylene-based separators and underscores the potential for practical applications in advanced energy storage technologies.

CRediT authorship contribution statement

S.M.B. Dissanayake: Writing – original draft, Validation, Software, Methodology, Investigation, Formal analysis, Data curation, Conceptualization. **I.G.K.J. Wimalasena:** Writing – original draft, Validation, Methodology, Investigation, Formal analysis, Data curation. **N.M. Keppetipola:** Software, Methodology, Data curation. **B.C. Karunarathne:** Software, Formal analysis. **A.D.T. Medagedara:** Software, Formal analysis. **Ludmila Cojocaru:** Writing – review & editing, Validation, Supervision. **Satoshi Uchida:** Writing – review & editing, Visualization, Validation. **R.M.G. Rajapakse:** Writing – review & editing, Validation, Supervision, Methodology. **Kirthi Tennakone:** Writing – review & editing, Validation, Supervision, Methodology, Conceptualization. **Masamichi Yoshimura:** Writing – review & editing, Visualization, Validation, Supervision, Funding acquisition, Conceptualization. **G.R.A. Kumara:** Writing – review & editing, Visualization, Validation, Supervision, Project administration, Investigation, Conceptualization.

Declaration of competing interest

The authors declare that they have no known competing financial interests or personal relationships that could have appeared to influence the work reported in this paper.

Acknowledgments

The authors would like to thank the National Institute of Fundamental Studies for providing facilities to carry out the research and to Condensed Matter & Solid-State Physics Research Group of the National Institute of Fundamental Studies for giving the Metrohm Autolab to analyze the fabricated supercapacitors, Philippe Legros (PLACAMAT) for SEM measurements and Marie-Anne Dourges (ISM, UMR 5255 CNRS) for her support for porosity calculation. Cojocaru L., Keppetipola N., thanks to the French government assistance, National Research Agency under the "Programme d'Investissements d'Avenir" with the reference "ANR-19-MPGA-0006". This study was also partly supported by the Research Center for the Smart Energy Technologies, Toyota Technological Institute, Japan.

References

[1] L. Miao, Z. Song, D. Zhu, L. Li, L. Gan, M. Liu, Recent advances in carbon-based supercapacitors, Mater. Adv. 1 (2020) 945–966, https://doi.org/10.1039/D0MA00384K.
[2] A. González, E. Goikolea, J.A. Barrena, R. Mysyk, Review on supercapacitors: technologies and materials, Renew. Sustain. Energy Rev. 58 (2016) 1189–1206, https://doi.org/10.1016/j.rser.2015.12.249.
[3] P. Sharma, T.S. Bhatti, A review on electrochemical double-layer capacitors, Energy Convers. Manag. 51 (2010) 2901–2912, https://doi.org/10.1016/j.enconman.2010.06.031.
[4] P. Mandake, P.B. Karandikar, Effect of separator thickness variation for supercapacitor with polyethylene separator material, Int. J. Sci. Res. Sci. Eng. Technol. 2 (2016) 967–971, https://doi.org/10.32628/IJSRSET1622232.
[5] B. Qin, Y. Han, Y. Ren, D. Sui, Y. Zhou, M. Zhang, Z. Sun, Y. Ma, Y. Chen, A ceramic-based separator for high-temperature supercapacitors, Energy Technol. 6 (2018) 306–311, https://doi.org/10.1002/ente.201700438.
[6] R. Arthi, V. Jaikumar, P. Muralidharan, Development of electrospun PVdF polymer membrane as separator for supercapacitor applications, Energy Sources, Part A Recovery, Util. Environ. Eff. 44 (2022) 2294–2308, https://doi.org/10.1080/15567036.2019.1649746.
[7] Q. Xie, X. Huang, Y. Zhang, S. Wu, P. Zhao, High performance aqueous symmetric supercapacitors based on advanced carbon electrodes and hydrophilic poly (vinylidene fluoride) porous separator, Appl. Surf. Sci. 443 (2018) 412–420, https://doi.org/10.1016/j.apsusc.2018.02.274.
[8] A. Laforgue, L. Robitaille, Electrochemical testing of ultraporous membranes as separators in mild aqueous supercapacitors, J. Electrochem. Soc. 159 (2012) A929–A936, https://doi.org/10.1149/2.020207jes.
[9] S. Banerjee, B. De, P. Sinha, J. Cherusseri, K.K. Kar, Applications of supercapacitors, in: Springer Series in Materials Science, Springer, Cham, 2020, pp. 341–350, https://doi.org/10.1007/978-3-030-43009-2_13.
[10] N.M. Keppetipola, M. Dissanayake, P. Dissanayake, B. Karunarathne, M. A. Dourges, D. Talaga, L. Servant, C. Olivier, T. Toupance, S. Uchida, K. Tennakone, G.R.A. Kumara, L. Cojocaru, Graphite-type activated carbon from

coconut shell: a natural source for eco-friendly non-volatile storage devices, RSC Adv. 11 (2021) 2854–2865, https://doi.org/10.1039/D0RA09182K.
[11] B. Szubzda, A. Szmaja, M. Ozimek, S. Mazurkiewicz, Polymer membranes as separators for supercapacitors, Appl. Phys. A 117 (2014) 1801–1809, https://doi.org/10.1007/s00339-014-8674-y.
[12] C. Schütter, S. Pohlmann, A. Balducci, Industrial requirements of materials for electrical double layer capacitors: impact on current and future applications, Adv. Energy Mater. 9 (2019) 1–11, https://doi.org/10.1002/aenm.201900334.
[13] D. Xu, G. Teng, Y. Heng, Z. Chen, D. Hu, Eco-friendly and thermally stable cellulose film prepared by phase inversion as supercapacitor separator, Mater. Chem. Phys. 249 (2020) 122979, https://doi.org/10.1016/j.matchemphys.2020.122979.
[14] I.M. Hauner, A. Deblais, J.K. Beattie, H. Kellay, D. Bonn, The dynamic surface tension of water, J. Phys. Chem. Lett. 8 (2017) 1599–1603, https://doi.org/10.1021/acs.jpclett.7b00267.
[15] J. Smithyman, A. Moench, R. Liang, J.P. Zheng, B. Wang, C. Zhang, Binder-free composite electrodes using carbon nanotube networks as a host matrix for activated carbon microparticles, Appl. Phys. Mater. Sci. Process 107 (2012) 723–731, https://doi.org/10.1007/S00339-012-6790-0/METRICS.
[16] A. Phaniendra, D.B. Jestadi, L. Periyasamy, Free radicals: properties, sources, targets, and their implication in various diseases, Indian J. Clin. Biochem. 30 (2015) 11–26, https://doi.org/10.1007/s12291-014-0446-0.
[17] H. Kaur, G. Hippargi, G.R. Pophali, A.K. Bansiwal, Treatment methods for removal of pharmaceuticals and personal care products from domestic wastewater, in: Pharmaceuticals and Personal Care Products: Waste Management and Treatment Technology, Elsevier, 2019, pp. 129–150, https://doi.org/10.1016/B978-0-12-816189-0.00006-8.
[18] A. Behera, B. Mittu, S. Padhi, N. Patra, J. Singh, Bimetallic nanoparticles: green synthesis, applications, and future perspectives, in: Multifunctional Hybrid Nanomaterials for Sustainable Agri-Food and Ecosystems, Elsevier, 2020, pp. 639–682, https://doi.org/10.1016/B978-0-12-821354-4.00025-X.
[19] M.N. Islam, M.H. Mahmoud, S. Mahbub, M.R. Islam, D. Kumar, A.Z. Ansari, S. Rana, M.A. Hoque, S.E. Kabir, Physico-chemical parameters and interaction forces associated with the clouding phenomenon of triton X-100 and ceftriaxone sodium mixture: an understanding of the impacts of potassium salts, Colloid Polym. Sci. 302 (2024) 213–224, https://doi.org/10.1007/S00396-023-05188-W/METRICS.
[20] H.A. Bhuiyan, J.M. Khan, D. Kumar, M.K. Banjare, R. Islam, S. Rana, A. Hoque, M. M. Rahman, S.E. Kabir, Phase separation, aggregation, and complexation of triton-X100 and bovine serum albumin mixture: a combined cloud point and UV–visible spectroscopic approaches, Int. J. Biol. Macromol. 269 (2024) 132184, https://doi.org/10.1016/J.IJBIOMAC.2024.132184.
[21] M.R.I. Rony, J.M. Khan, M.R. Islam, K.M.K. Alam, D. Kumar, A. Ahmad, S. Rana, M. A. Hoque, Exploration of phase separation and several physicochemical parameters of the mixture of triton X-100 and ceftriaxone sodium salt: influences of the composition of sodium salts, Chem. Pap. 78 (2023) 307–319, https://doi.org/10.1007/S11696-023-03085-8.
[22] S.M.R. Islam, M.R. Islam, S. Mahbub, K. Hasan, D. Kumar, J.M. Khan, A. Ahmad, M. A. Hoque, D.M.S. Islam, Impacts of hydrotropes on clouding phenomena and physico-chemical parameters coupled with the triton X 100 & promethazine hydrochloride mixture, Mol. Phys. 121 (2023) e2212535, https://doi.org/10.1080/00268976.2023.2212535.
[23] M.R. Alam, M.R. Islam, J.M. Khan, U. Rayhan, S. Rana, D. Kumar, A. Ahmad, M. A. Hoque, S.E. Kabir, Physicochemical investigations of clouding development and physicochemical properties of Triton X-100 and levofloxacin hemihydrate mixture: influence of sodium salts composition, Colloid Polym. Sci. 301 (2023) 1125–1136, https://doi.org/10.1007/S00396-023-05132-Y/METRICS.
[24] M.R.I. Rony, J.M. Khan, I. Jahan, M.T.R. Joy, T. Hasan, D. Kumar, A. Ahmad, S. Rana, M.A. Hoque, Influences of alcohols, urea and polyethylene glycol on the cloudy formation nature and physico-chemical parameters of the mixture of triton X-100 and ceftriaxone sodium salt, Colloids Surf. A Physicochem. Eng. Asp. 677 (2023) 132410, https://doi.org/10.1016/J.COLSURFA.2023.132410.
[25] M. Nazrul Islam, M. Abdul Rub, M. Rafikul Islam, M. Abdul Goni, S. Rana, D. Kumar, A.M. Asiri, Y.G. Alghamdi, M. Anamul Hoque, S.E. Kabir, Physico-chemical study of the effects of electrolytes and hydrotropes on the clouding development of TX-100 and ceftriaxone sodium drug mixture, J. Mol. Liq. 379 (2023) 121601, https://doi.org/10.1016/J.MOLLIQ.2023.121601.
[26] Z. Liu, Y. Zhang, Y. Sang, Z. Nie, Scalable synthesis of ultrasmall hybrid silica colloidal particles through balanced solvophobic interaction and electrostatic repulsion, Colloid Polym. Sci. 302 (2024) 1209–1217, https://doi.org/10.1007/s00396-024-05258-7.
[27] G. Wang, H. Wang, B. Zhong, L. Zhang, J. Zhang, Supercapacitors' Applications, Taylor & Francis Group, LLC, 2016, pp. 479–492.
[28] J. Liu, F. Mirri, M. Notarianni, M. Pasquali, N. Motta, High performance all-carbon thin film supercapacitors, J. Power Sources 274 (2015) 823–830, https://doi.org/10.1016/j.jpowsour.2014.10.104.
[29] X. Du, S. Wang, Y. Liu, M. Lu, K. Wu, M. Lu, Self-assembly of free-standing hybrid film based on graphene and zinc oxide nanoflakes for high-performance supercapacitors, J. Solid State Chem. 277 (2019) 441–447, https://doi.org/10.1016/j.jssc.2019.06.003.
[30] K.P.S. Prasad, D.S. Dhawale, T. Sivakumar, S.S. Aldeyab, J.S.M. Zaidi, K. Ariga, A. Vinu, Fabrication and textural characterization of nanoporous carbon electrodes embedded with CuO nanoparticles for supercapacitors, Sci. Technol. Adv. Mater. 12 (2011) 044602, https://doi.org/10.1088/1468-6996/12/4/044602.
[31] Y. Chen, X. Zhang, H. Zhang, X. Sun, D. Zhang, Y. Ma, High-performance supercapacitors based on a graphene–activated carbon composite prepared by chemical activation, RSC Adv. 2 (2012) 7747, https://doi.org/10.1039/c2ra20667f.
[32] J. Zhao, A.F. Burke, Review on supercapacitors: technologies and performance evaluation, J. Energy Chem. 59 (2021) 276–291, https://doi.org/10.1016/j.jechem.2020.11.013.
[33] Y. Zhigalenok, S. Abdimomyn, K. Zhumadil, M. Lepikhin, A. Starodubtseva, M. Kiyatova, N. Shpigel, F. Malchik, A practical guide for separator selection, characterization, and electrochemical evaluation for supercapacitor application, Appl. Phys. Rev. 11 (2024) 031315, https://doi.org/10.1063/5.0202782.
[34] S. Verma, S. Verma, S. Kumar, B. Verma, Multidimensional Nanomaterials for Supercapacitors: Next Generation Energy Storage, 2024, pp. 1–364, https://doi.org/10.2174/9789815223408124010l.
[35] J. Zhang, M. Gu, X. Chen, Supercapacitors for renewable energy applications: a review, Micro Nano Eng. 21 (2023) 100229, https://doi.org/10.1016/J.MNE.2023.100229.
[36] S. Rani, N. Kumar, Y. Sharma, Recent progress and future perspectives for the development of micro-supercapacitors for portable/wearable electronics applications, J. Phys.: Energy 3 (2021) 032017, https://doi.org/10.1088/2515-7655/ac01c0.
[37] S.R. Salkuti, Advanced technologies for energy storage and electric vehicles, Energies 16 (2023) 2312, https://doi.org/10.3390/en16052312.
[38] C.Y. Bon, L. Mohammed, S. Kim, M. Manasi, P. Isheunesu, K.S. Lee, J.M. Ko, Flexible poly(vinyl alcohol)-ceramic composite separators for supercapacitor applications, J. Ind. Eng. Chem. 68 (2018) 173–179, https://doi.org/10.1016/J.JIEC.2018.07.043.
[39] U. Jadli, F. Mohd-Yasin, H.A. Moghadam, J.R. Nicholls, P. Pande, S. Dimitrijev, The correct equation for the current through voltage-dependent capacitors, IEEE Access 8 (2020) 98038–98043, https://doi.org/10.1109/ACCESS.2020.2997906.
[40] A. Patist, S.G. Oh, R. Leung, D.O. Shah, Kinetics of micellization: its significance to technological processes, Colloids Surf. A Physicochem. Eng. Asp. 176 (2001) 3–16, https://doi.org/10.1016/S0927-7757(00)00610-5.
[41] O. Segun Esan, Effect of micellar aggregate on the kinetics and mechanism of the reaction between ethylene glycol and periodate, Int. Sch. Res. Notices (2014) (2014) 1–3, https://doi.org/10.1155/2014/680176.
[42] S. Buller, E. Karden, D. Kok, R.W. De Doncker, Modeling the dynamic behavior of supercapacitors using impedance spectroscopy, IEEE Trans. Ind. Appl. 38 (2002) 1622–1626, https://doi.org/10.1109/TIA.2002.804762.